URSI GASS 2023, Sapporo, Japan, 19 – 26 August 2023

Formation of zebra stripes of electrons in response to the intensification of Region 1 field-aligned currents

Megha Pandya*(1), Yusuke Ebihara(1), Takashi Tanaka(2), and Jerry W. Manweiler(3)
(1) Research Institute for Sustainable Humanosphere, Kyoto University, Uji, Japan. ; e-mail: pandya.meghamahendra.3j@kyoto-u.ac.jp; ebihara@rish.kyoto-u.ac.jp
(2) International Research Center for Space and Planetary Environmental Science, Kyoto University, Uji, Japan.; e-mail: takashi.tanaka.084@m.kyushu-u.ac.jp;
(3) Fundamental Technologies, LLC, Lawrence, KS, USA. e-mail: Jerry.Manweiler@ftecs.com

Abstract

Electron "zebra stripes" are band-like structures observed in energetic electron spectrograms having quasi-periodic peaks and valleys in their flux intensities. This is the first study that couples the MHD simulation with a test particle to address (i) the mechanism for the formation of zebra stripes, and (ii) the preferential location of the origin of the peaks in the zebra patterns. To determine the distribution of electron fluxes in the inner magnetosphere, we use the advection simulation under the time-dependent ionospheric electric fields provided by the global magnetohydrodynamics (MHD) simulation. Using simulation, we delineate the fundamental properties of the electron zebra stripes that have been recorded by the Radiation Belt Storm Probes Ion Composition Experiment (RBSPICE) instrument on board Van Allen Probe-A during the geomagnetic storm of 7-8 September 2017. At the start of the simulation, smooth and monotonic distribution of the electron fluxes appear, which transforms into zebra patterns under the influence of westward electric field pulses in the premidnight-postdawn region. Therefore, electrons forming the peaks move inward due to the EXB electric field that is intensified in the westward direction. On the other hand, the valley electrons have no significant inward motion. Interestingly, the net magnitude of the upward-flowing FACs intensifies during the westward turning of the electric field. Thus, the electron zebra stripes are the consequence of the solar wind magnetosphere coupling via the ionosphere giving electron flux distribution that has and has not undergone radially inward motion.

1 Introduction

The radiation belts are torus-shaped regions in the Earth's magnetosphere that mainly comprises energetic electrons and ions. The electron population is divided into two zones: the outer radiation belt (~4–5 R_E) and the inner radiation belt (<2.5 R_E) in the equatorial plane. A region of low electron flux is called a "slot" that separates the outer electron radiation belt from an inner zone. In the inner belt, periodic peaks and valleys in the electron flux intensities are observed in the energy versus *L*-value spectra. These features are named "zebra stripes" [1]. The difference in the electron flux intensities between the peaks and valleys is of the order of one or more. At the beginning of the space era, these features were reported near the South Atlantic Anomaly region by low-altitude, polar-orbiting satellites [2-4]. With the development of space technology, it was found that such structures can be observed at L<3 during geomagnetically quiet and disturbed intervals [5-6].

Numerous studies have been proposed to explain the formation of electron zebra stripes, but it remains still unresolved. In the early days, it was observed that the peaks in the electron zebra stripes are the consequence of the drift-resonant mechanism that accelerates and decelerates the electrons with specific energies. However, Cladis [7] proposed that the source of electromagnetic fluctuations could be associated with the periodic variations in the ionospheric currents. Contrarily, Sauvad et al. [6] showed that the long-period ULF waves could be responsible for the peaks observed during enhanced geomagnetic activity. Recently, Ukhorskiy et al. [1] developed a model and postulated that the electric field induced due to the corotation of the Earth is responsible for the formation of the quiet time electron zebra stripes. A number of studies invoking the electric field models have been suggested to explain the formation of electron zebra stripes but it still remains unsolved. Also, there are no clear studies that explain the preferential location of the origin of these peaks. Our studies involve a detailed analysis of the results obtained from the advection simulation and MHD simulation. A comparison is made with the satellite-based observations to understand its variability with time. Our computer simulation results provide a detailed overview of the formation mechanism and preferential location for the origin of electron zebra stripes in the Earth's inner magnetosphere.

2 Data and Simulation details:

To exclusively study the energetic electrons in the Earth's radiation belts the Van Allen Probes satellite was launched in the year 2012. It flies in the near-equatorial region with an orbital period of ~9 h with perigee at ~700 km, an apogee at ~6.2 R_E [8]. We obtain the electron fluxes in the energy range of 20 keV- 938 keV recorded by Radiation Belt Storm Probes Ion Composition

Instrument (RBSPICE) [9] aboard NASA's Van Allen Probe-A spacecraft.

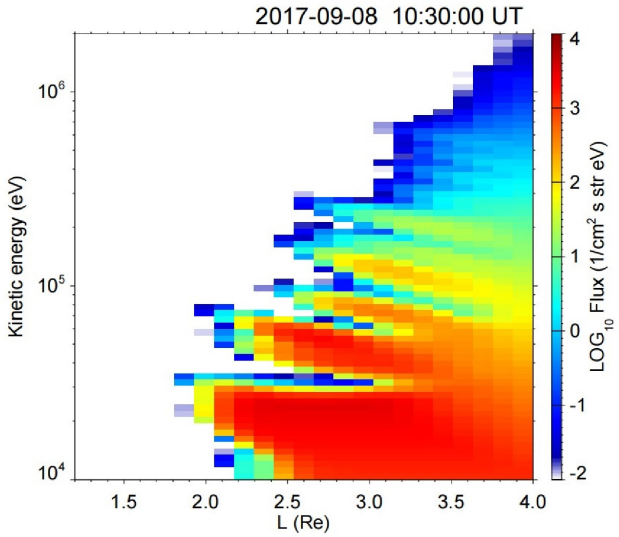

Figure 1. Energy versus *L*-value spectrogram of the simulated electron fluxes in the Earth's inner magnetosphere on 8 September 2017. The abscissa is the distance from the centre of the Earth (in Earth-radii), and the ordinate is the kinetic energy of the electrons.

Apart from satellite measurements, we employed advection simulation to reproduce these zebra patterns and understand their evolution under the influence of the electric fields obtained from the global Magnetohydrodynamic (MHD) simulation. To obtain a detailed understanding of the distribution of the electron fluxes in the Earth's inner magnetosphere, we solve the following advection equation

$$\frac{\partial f}{\partial t}+\frac{1}{RS_b}\frac{\partial}{\partial R}\left(RS_b\left\langle\frac{dR}{dt}\right\rangle f\right)+\frac{1}{S_b}\frac{\partial}{\partial\varphi}\left(S_b\left\langle\frac{d\varphi}{dt}\right\rangle f\right)$$
$$+\frac{1}{\gamma p}\frac{\partial}{\partial K}\left(\gamma p\left\langle\frac{dK}{dt}\right\rangle f\right)+\frac{1}{xS_b}\frac{\partial}{\partial x}\left(xS_b\frac{dx}{dt}f\right)=\left(-\frac{2f}{\tau_b}\right)_{\text{loss cone}}, \quad (1)$$

where f, R, S_b, φ, K, x, p, γ and t_b are the phase space density of electrons, the distance from the center of the Earth, half-bounce path length, the magnetic local time (MLT), the kinetic energy, cosine of the equatorial pitch angle, the momentum of a particle, the Lorentz factor, and the bounce period, respectively. The magnetosphere is empty at the beginning of the simulation and the magnetic field is assumed to be dipolar in nature. The time-varying electric fields required for the advection simulation are provided by the global MHD simulation. Detailed information about the global MHD simulation can be obtained from Tanaka [10]. To obtain the characteristics of the electron zebra stripes, we back-trace the electron trajectory using the test particle simulation.

3 Observations and Analysis

On 8 September 2017, Radiation Belt Storm Probes Ion Composition Experiment (RBSPICE) instrument onboard Van Allen Probe-A recorded zebra stripes in the energy range of 20-500 keV, below *L*=2.5. The electron zebra stripes get distorted during the geomagnetic storm main phase and reappeared after the storm has passed (not shown). Using simulations, we reproduce the peaks and valleys in the energy versus *L*-value spectrogram that resembles observed zebra patterns. Figure 1 shows the simulated electron zebra stripes at 0000 MLT and 1030 UT on 8 September 2017 for 67.7° equatorial pitch angle.

To fetch the properties of the simulated peaks in the electron zebra stripes the electron trajectories are traced backward in time from the point at *L*=3 and midnight at 1030 UT on 8 September 2017. Figure 2 (a-d) shows the properties of the electrons with different energies that give rise to the peaks and valleys in the electron fluxes. The color code represents the electrons with different energies. As shown in Figure 2a, the electrons forming the peaks reach the outer boundary of *L*=4, while the electrons forming valleys do not. The peak-forming electrons start to move inward when the azimuthal component of the electric field is westward (Figure 2b). Our simulation results indicate that electrons forming the peaks do not enter from all the MLT but follow a specific MLT dependence. A significant inward transport of the electrons is observed during the premidnight-postdawn region (Figure 2c). During the inward transport, the electrons gain energy as shown in Figure 2d. The net magnitude of the field-aligned currents (FACs) remains at a high from ~2300 UT on 7 September to ~0200 UT on 8 September 2017. During the interval of enhanced FACs, the electron forming the peaks in the zebra stripes moved radially inward. Contrarily, the electrons forming the valleys do not come from the outer boundary (Figure 2a).

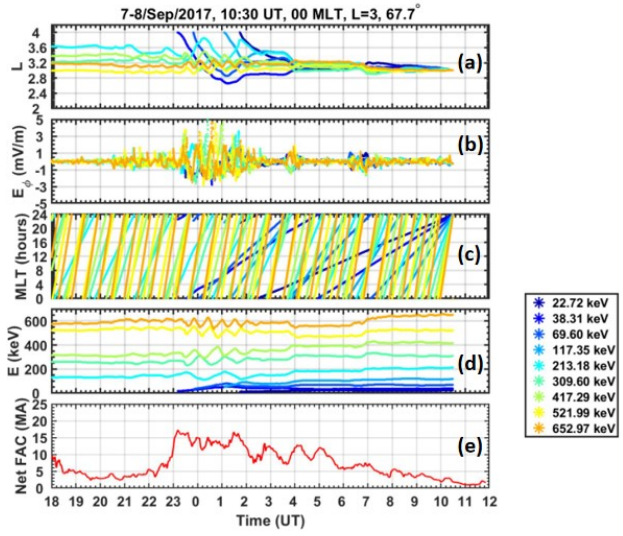

Figure 2 Back-tracing of the electron trajectories starting at 1030 UT and *L*=3 on 8 September 2017. The color code in the *L*-value (a), an azimuthal component of electric field (b), MLT (c), and kinetic energies (d) show the initial energies of the electrons, while the initial pitch angle is 67.7°. Panel (e) shows the net magnitude of the

field-aligned currents (FACs) obtained from the global MHD simulation.

To infer the mechanism for the formation of electron zebra stripes and reasons for the specific MLT dependence, we show the *L*-MLT distributions of the magnetospheric conditions starting from 1030 UT on 8 September 2017 (Figure 3). As shown in Figure 3(a), at 1030 UT, two pairs of the Field Aligned Currents (FACs) are observed. The inward pair corresponds to Region-1, and the outward pair corresponds to the Region-2 FACs. During this interval, an enhanced ionospheric conductivity is observed (panel b) that shows a strong gradient around the midnight region. The ionospheric conductivity represents the auroral oval. The ionospheric potential contours also grow and become asymmetric (panel c). The ionospheric potential contours intensify and spread across the equatorward edge. The negative electric potential (blue) deforms and extends to the dawnside at the lower latitudes. The elongation of the duskside cell results in the generation of a strong electrical field (panel d). After this period of time, the intensity of the Region-1 FACs decreases and the conductivity, the ionospheric potentials, and hence ionospheric electric fields also decrease (not shown).

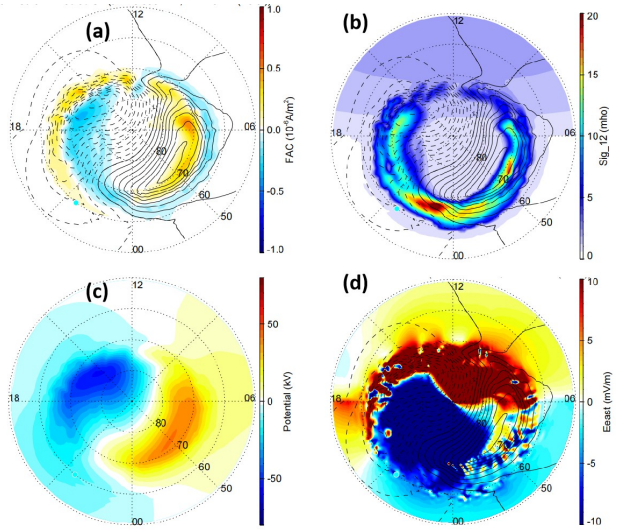

Figure 3 Panels (a-d) shows the distributions of (a) field aligned currents (FACs), (b) the ionospheric Hall conductivity, (c) the electric potential (positive indicated by red and negative potentials are indicated by blue), and (d) east (red) and west (blue) component of the ionospheric electric field in the ionosphere in the Northern Hemisphere at 1030 UT on 8 September 2017.

4 Discussion

Long ago, Cladis [7] indicated that geomagnetic field fluctuations at lower altitudes are probably the outcome of local ionospheric currents. In response to the increased interaction between the magnetosheath and the magnetospheric plasma, the magnetospheric convection begins that drives an electrical current called Region-1 FACs connecting the Earth's magnetosphere and the ionosphere [11]. Ebihara et al. [12] made extensive efforts to explain the generation of Region-1 FACs. They found that the Region-1 FACs are likely to be generated in the low-latitude magnetopause where the southward component of the IMF leads to the reconnection process and the magnetospheric magnetic field lines are dragged in the anti-sunward direction by the magnetospheric and solar wind-originated plasma leading to the formation of region-1 FACs. At high latitudes, the FAC gives rise to the twin vortex pattern of the ionospheric convection cell patterns (electric potential pattern). The gradient in the ionospheric conductivity leads to a negative space charge accumulated at the equatorward edge of the nightside auroral oval increases that elongate the duskside convection cell to the dawnside.. Therefore, the westward component of the electric field gets shifted to the dawnside. Also, figure 2e shows the important role of FACs in driving the azimuthal electric fields. The magnitude of net FACs is high when the convection electric field turns westward. The field aligned currents play a major role in controlling the magnitude and direction of the electric fields. The role of electric fields in driving the zebra stripes is consistent with the observational studies made by Lejosne and Mozer [13] that highlights the role of electric fields in the formation of electron zebra stripes. The westward electric field also imposes a radially inward motion due to EXB drift. Thus, the gradient in the conductivity could be responsible for the skew of the potential contours and hence the formation of the westward electric field, which is consistent with the observations made by Lejosne and Mozer [13].

5 Summary

In our studies, we analyze the energy versus *L*-value spectrum for the electrons in the energy range of 0.02-0.95 MeV recorded by the Radiation Belt Storm Probes Ion Composition Experiment (RBSPICE) onboard Van Allen Probes. A clear electron zebra distribution is observed on 8 September 2017. We invoked the simulation-based approach to understand the mechanism responsible for the formation of the electron zebra stripes. The major outcome of our studies are:

- The electrons comprising the peaks of the zebra stripes come from the outer region where the phase space density of the electrons is high.
- The magnitude of net FACs is closely associated with the azimuthal electric fields.
- A strong gradient in the ionospheric conductivity is observed in the midnight region, leading to the skewing of the duskside potential contours to the dawnside. During this process, a strong westward component of the azimuthal electrical field appears.
- The electrons comprising the peaks in the zebra stripes preferentially move inward in the pre-midnight to the dusk sector where the westward electric field is significantly enhanced.

Thus, the electrons giving rise to the peaks and valleys in the zebra stripes are generated at different azimuthal locations. A sudden change in electric fields over a period less than the drift period of electrons plays an important role in the generation of the zebra stripes. The magnitude of net FACs also poses an interesting question for the future: What is the effect of the magnitude of FACs in driving the dynamics of the inner belt electrons and hence zebra stripes? This will be our next step for future studies where we will highlight the importance of magnetosphere-ionosphere coupling in driving plasma dynamics.

Acknowledgements

The RBSPICE data used in this study are available from (http://rbspice.ftecs.com/Data.html). We acknowledge the use of OMNI data and NASA/GSFC's Space Physics Data Facility's OMNIWeb (https://omniweb.gsfc.nasa.gov/) service.

References

[1] A. Ukhorskiy, M. I. Sitnov, D. G. Mitchell, K. Takahashi, L. J. Lanzerotti, & B. H. Mauk, Rotationally driven `zebra stripes' in Earth's inner radiation belt. Nature, 507 (7492), 338–340. https://doi.org/10.1038/nature13046, 2014.

[2] W. L. Imhof & R. V. Smith, Observation of nearly monoenergetic high-energy electrons in the inner radiation belt. Physical Review Letters, 14(22), 885. https://doi.org/10.1103/physrevlett.14.885, 1965.

[3] W. L. Imhof & R. V. Smith, Low altitude measurements of trapped electrons. In Radiation Trapped in the Earth's Magnetic Field (pp. 100–111). Springer, 1966.

[4] W. L. Imhof, E. E. Gaines, & J. B. Reagan, Dynamic variations in intensity and energy spectra of electrons in the inner radiation belt. Journal of Geophysical Research, 78(22), 4568–4577. https://doi.org/10.1029/ja078i022p04568, 1974.

[5] D. W. Datlowe, W. L. Imhof, E. E. Gaines & H. D. Voss, Multiple peaks in the spectrum of inner belt electrons. Journal of Geophysical Research, 90(A9), 8333. https://doi.org/10.1029/ja090ia09p08333, 1986.

[6] J.-A. Sauvaud, M. Walt, D. Delcourt, C. Benoist, E. Penou, Y. Chen, & C. T. Russell, Inner radiation belt particle acceleration and energy structuring by drift resonance with ULF waves during geomagnetic storms. Journal of Geophysical Research: Space Physics, 118(4), 1723–1736. https://doi.org/10.1002/jgra.50125, 2013.

[7] J. B. Cladis, Resonance acceleration of particles in the inner radiation belt. In Radiation Trapped in the Earth's Magnetic Field (pp. 112–115). Springer. https://doi.org/10.1007/978-94-010-3553-8_9, 1966.

[8] B. H. Mauk, N. J. Fox, S. G. Kanekal, R. L. Kessel, D. G. Sibeck, & A. Ukhorskiy, Science Objectives and Rationale for the Radiation Belt Storm Probes Mission. Space Science Reviews, 179(1–4), 3–27. https://doi.org/10.1007/s11214-012-9908-y, 2013.

[9] D. G. Mitchell, L. J. Lanzerotti, C. K. Kim, M. Stokes, S. Cooper, A. Ukhorskiy, J. W. Manweiler, S. Jaskulek, D. K. Haggerty, P. Brandt, M. Sitnov, K. Keika, J. R. Hayes, L. E. Brown, R. S. Gurnee, R. S. Hutcheson, J. C. Nelson, K. S. Paschalidis, et al. Radiation Belt Storm Probes Ion Composition Experiment (RBSPICE). Space Science Reviews, 179(1–4), 263–308. https://doi.org/10.1007/s11214-013-9965-x, 2015.

[10] T. Tanaka, Substorm Auroral Dynamics Reproduced by Advanced Global Magnetosphere−Ionosphere (M–I) Coupling Simulation, edited, pp. 177-190, doi:10.1002/9781118978719.ch13, 2015.

[11] G. L. Siscoe, G. M. Erickson, B. U. Sonnerup, et al., Hill model of transpolar potential saturation: Comparisons with MHD simulations, J. Geophys. Res. 107(A6), doi:10.1029/2001JA000109, 2002.

[12] Y. Ebihara, & T. Tanaka, Where Is Region 1 Field-Aligned Current Generated? Journal of Geophysical Research: Space Physics, 127(3). https://doi.org/10.1029/2021ja029991, 2022

[13] S. Lejosne, & F. S. Mozer, Experimental Determination of the Conditions Associated With Zebra Stripe Pattern Generation in the Earths Inner Radiation Belt and Slot Region. Journal of Geophysical Research: Space Physics, 125(7). https://doi.org/10.1029/2020ja027889, 2020.